Received 29 June 2020; accepted 12 July 2020. Date of publication 15 July 2020; date of current version 31 July 2020.

Digital Object Identifier 10.1109/OJCOMS.2020.3009386

Space Division Multiple Access With Distributed User Grouping for Multi-User MIMO-VLC Systems

CHEN CHEN [1] (Member, IEEE), YANBING YANG [2] (Member, IEEE), XIONG DENG [3] (Member, IEEE), PENGFEI DU [4], AND HELIN YANG [5] (Member, IEEE)

[1]School of Microelectronics and Communication Engineering, Chongqing University, Chongqing 400044, China

[2]College of Computer Science, Sichuan University, Chengdu 610065, China

[3]Department of Electrical Engineering, Eindhoven University of Technology (TU/e), 5600 MB Eindhoven, The Netherlands

[4]A*STAR's Singapore Institute of Manufacturing Technology, Singapore 138634

[5]School of Electrical and Electronic Engineering, Nanyang Technological University, Singapore 639798

CORRESPONDING AUTHOR: C. CHEN (e-mail: c.chen@cqu.edu.cn)

This work was supported by the National Natural Science Foundation of China under Grant 61901065. A part of this paper was published in IEEE Global Communications Conference, Waikoloa, HI, USA, Dec. 2019 [33].

ABSTRACT To support multiple users in an indoor multiple-input multiple-output visible light communication (MIMO-VLC) system adopting spatial multiplexing, orthogonal frequency division multiple access (OFDMA) is usually adopted, where the overall modulation bandwidth is shared by all the users. In this paper, by fully exploiting the spatial distributions of light-emitting diode (LED) transmitters in the ceiling and end users around the receiving plane, we propose a space division multiple access (SDMA) technique for indoor spatial multiplexing-based MIMO-VLC systems. When applying SDMA, users within the MIMO-VLC system are divided into different user groups (UGs) based on their spatial locations with respect to different LED transmitters. Specifically, each UG can use the overall modulation bandwidth of the system. For efficient implementation of SDMA, two distributed user grouping (DUG) approaches are proposed, including basic DUG and transmit diversity-enhanced DUG (TD-DUG), and a two-step resource allocation algorithm is further designed. The achievable rates of the MIMO-VLC system employing SDMA with both basic DUG and TD-DUG are derived accordingly. To verify the superiority of SDMA over conventional OFDMA, detailed analytical and simulation results are presented. Moreover, a proof-of-concept experiment is conducted to demonstrate the advantage of SDMA in a practical spatial multiplexing-based MIMO-VLC system.

INDEX TERMS Distributed user grouping (DUG), multiple-input multiple-output (MIMO), space division multiple access (SDMA), visible light communication (VLC).

I. INTRODUCTION

IT IS predicted that light-emitting diodes (LEDs) will gradually replace conventional incandescent and fluorescent lamps for indoor lighting and become the dominator of the global illumination market in the near future. The wide application of white LEDs for indoor illumination is due to their many inherent advantages such as high energy efficiency, long lifetime, enhanced tolerance against humidity, limited heat generation, low cost and small size [1]. Besides illumination, white LEDs can also be switched on and off at a relatively high speed such that human eyes cannot perceive the changes in light intensity, but a perceptive photodetector can detect and interpret the light intensity variations. Consequently, visible light communication (VLC), which explores LEDs to transmit data and meanwhile maintains their primary function of illumination, has been proposed and extensively investigated in recent years [2]–[4]. VLC has been envisioned as a promising complementary technology to traditional radio-frequency (RF) technologies. By exploiting high-speed, bidirectional and networked VLC systems,

light-fidelity (LiFi) can be deployed in typical indoor environments [5]. Compared with traditional RF technologies such as wireless-fidelity (WiFi), VLC/LiFi enjoys many exiting advantages such as huge and unregulated spectrum, potentially high data rate, low-cost front-ends and no electromagnetic interference (EMI) [6]. Leveraging the dual-use of LEDs for simultaneous indoor illumination and wireless communication, many other emerging applications of VLC has been reported, such as positioning and localization, sensing, object ranging and detecting, and so on [7]–[9].

Although white LEDs have abundant unregulated spectrum ranging from about 380 to 780 nm, the practically available 3-dB modulation bandwidth of commercial off-the-shelf (COTS) white LEDs is usually very small, especially for the phosphor-coated white LEDs which is only about several MHz [10]. As a result, it is quite challenging to achieve high-speed and large-capacity VLC systems by utilizing low-cost COTS white LEDs. To overcome the bandwidth limitation, many capacity-enhancing techniques have been proposed for VLC systems using COTS white LEDs so far, including frequency domain equalization (FDE) schemes for substantial extension of LED modulation bandwidth [11]–[13], spectral-efficient modulation formats such as orthogonal frequency division multiplexing (OFDM) using high-order quadrature amplitude modulation (QAM) constellations [14], [15], and multiple-input multiple-output (MIMO) transmission [16], [17]. In particular, MIMO is a very natural and efficient way to improve the achievable capacity of an indoor VLC system, since multiple LEDs are commonly mounted in the ceiling of a typical indoor environment so as to obtain sufficient and uniform illumination [18]. Conventional MIMO transmission techniques mainly include repetition coding, spatial multiplexing and spatial modulation [19]. Among them, spatial multiplexing is one of the most widely adopted MIMO transmission techniques in bandlimited MIMO-VLC systems due to its high spectral efficiency [16], [20]. Moreover, MIMO-VLC systems can be generally divided into two categories based on the type of the adopted optical lens: one is non-imaging MIMO which might suffer from high inter-channel interference (ICI) [16], [17], and the other is imaging MIMO which utilizes specially designed imaging receivers to eliminate ICI [21]–[23]. Although imaging MIMO can achieve negligible ICI, its performance largely depends on the specific lens design of the imaging receiver, which inevitably increases the complexity and cost of MIMO-VLC systems [24]. In the following, MIMO is specifically referred to non-imaging MIMO applying spatial multiplexing.

In a practical indoor MIMO-VLC system, there might be more than one user within the system coverage and hence an efficient multiple access scheme should be adopted to support multiple users simultaneously. To date, several schemes have been reported in literature. In [25], [26], precoding techniques have been applied in multiuser MIMO-VLC systems, which can help to remove multi-user interference (MUI) and hence separate the received signals for different users. Nevertheless, since COTS white LEDs usually have a very limited dynamic range and suffer from severe LED nonlinearity, the practical implementation of precoding might be quite challenging [27]. As a multiple access scheme generated from OFDM, orthogonal frequency division multiple access (OFDMA) has already been applied in multiuser VLC systems [28], [29], where the overall modulation bandwidth of the system is divided and shared by all the users. However, the available bandwidth of each individual user becomes relatively small due to spectrum partitioning, which inevitably leads to reduced achievable rate, especially when the VLC system is expected to support a large number of users.

Lately, the space division multiple access (SDMA) technique has been proposed for multiuser VLC systems. In [30], SDMA based on optical beamforming was proposed, which has high implementation complexity due to the use of a LED light, a spatial light modulator (SLM) and a LED/SLM controller. In [31], SDMA was achieved by substituting the conventional single-element LED transmitter with a well-designed angle diversity transmitter, which has a relatively complicated structure consisting of multiple directional narrow-beam LED elements. In [32], an adaptive Walsh-Hadamard transform spreading-assisted SDMA-OFDM scheme was proposed to enhance multi-user downlink capability in multiuser MIMO-VLC systems, where SDMA was achieved by using an imaging receiver. In brief, the state-of-the-art SDMA techniques proposed for multiuser VLC or MIMO-VLC systems are mainly based on the use of specially designed transceiver structures, which inevitably increase complexity and cost.

In this paper, we propose a SDMA technique for multiuser MIMO-VLC systems, without using specially designed transceiver structures. The preliminary results were presented in the IEEE Global Communications Conference (GLOBECOM), 2019 [33]. The proposed SDMA aims to improve the available bandwidth of each user and hence enhance the achievable rate of the MIMO-VLC system, while keeping the implementation complexity as low as possible. The main contributions of this work are summarized as follows:

- A novel SDMA technique is proposed to simultaneously support multiple users in an indoor single-cell multiuser MIMO-VLC system, where users within the system can be efficiently divided into different user groups (UGs), according to the distinctive spatial positions of the ceiling LEDs and the relative positions of users with respect to different LEDs. Consequently, each UG can utilize the overall modulation bandwidth of the system.
- Two distributed user grouping (DUG) approaches are proposed for efficient user grouping in SDMA-enabled MIMO-VLC systems, which can be easily implemented by evaluating the signal-to-noise ratio (SNR) performance of the users within the system.
- A two-step resource allocation algorithm is designed for MIMO-VLC systems employing SDMA with DUG,

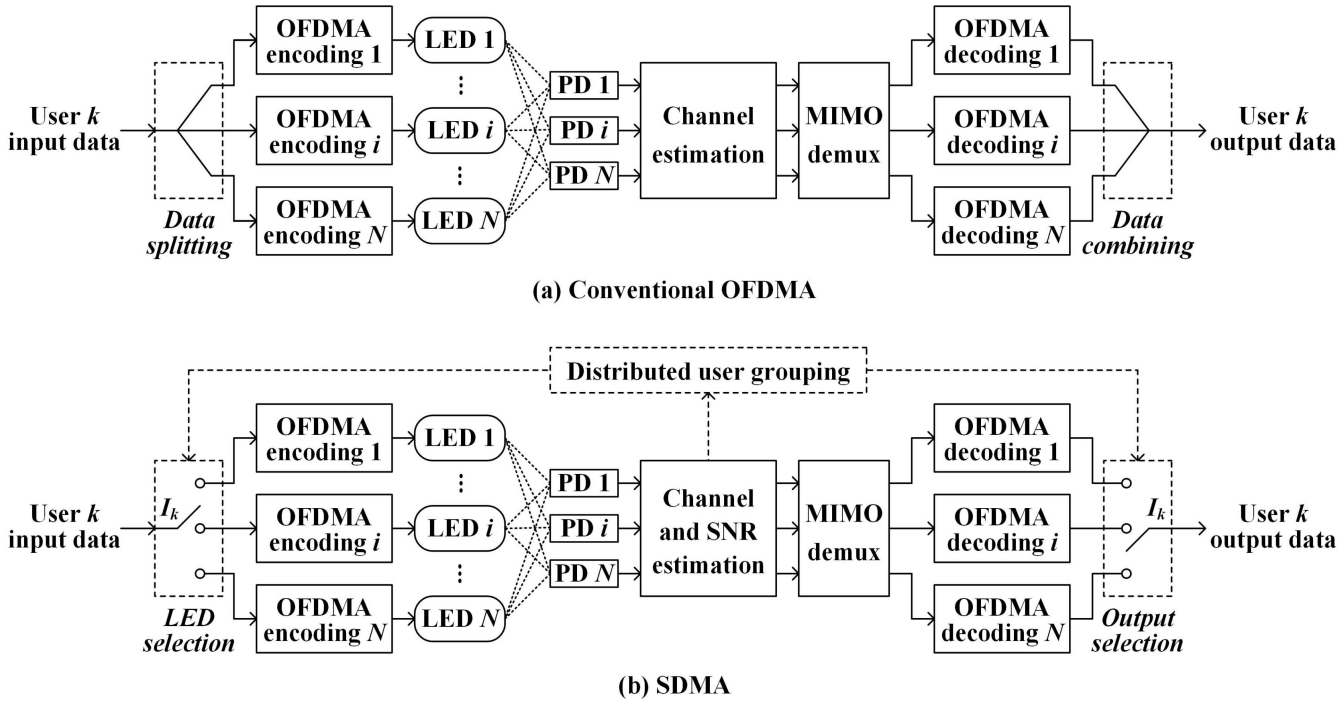

FIGURE 1. Schematic diagram of a single-cell K-user $N \times N$ MIMO-VLC system using (a) conventional OFDMA and (b) SDMA with distributed user grouping. Only the k-th user is shown for illustration.

which involves both inter-UG space allocation and intra-UG subcarrier allocation.
- Based on the obtained detailed analytical, simulation and experimental results, we successfully verify the superiority of SDMA over conventional OFDMA in terms of the achievable sum rate of MIMO-VLC systems.

The rest of this paper is organized as follows. Sections II and III describe the model of an indoor multiuser MIMO-VLC system using conventional OFDMA and the proposed SDMA, respectively. Analytical and simulation results are presented in Section IV and experimental results are provided in Section V. Finally, Section VI concludes the paper.

Notation: $(\cdot)^T$, $(\cdot)^*$ and $(\cdot)^\star$ represent the transpose, conjugated transpose and pseudo inverse of a vector or matrix, respectively. $(\cdot)^{-1}$ denotes the inverse of a matrix. Non-boldface italic letters, lowercase boldface letters and capital boldface letters represent scalars, vectors and matrices, respectively.

II. MIMO-VLC USING CONVENTIONAL OFDMA

In this section, we first describe the mathematical model of an indoor multiuser MIMO-VLC system using conventional OFDMA. It is assumed that there are totally N LEDs mounted in the ceiling and K users randomly located over the receiving plane, where each user is assumed to be equipped with N photodiodes (PDs) which are vertically oriented towards the ceiling. For simplicity and without loss of generality, the system is assumed to have a flat frequency response with an overall modulation bandwidth of B. Moreover, DC-biased optical OFDM (DCO-OFDM) modulation is adopted in the MIMO-VLC system [34]. Then, we further analytically derive the achievable rate of each user and the achievable sum rate of all the K users in the MIMO-VLC system using conventional OFDMA.

A. PRINCIPLE OF CONVENTIONAL OFDMA

Fig. 1(a) depicts the schematic diagram of an indoor single-cell K-user $N \times N$ MIMO-VLC system using conventional OFDMA, where only the k-th ($k = 1, 2, \ldots, K$) user is shown for illustration. By applying conventional OFDMA, the overall modulation bandwidth of the system is divided into K subbands and each user is allocated with one subband for signal transmission. The corresponding resource allocation scheme for conventional OFDMA is shown in Fig. 2(a). In this work, we assume that each user is allocated with an equal number of data subcarriers, i.e., bandwidth, and also an equal transmit electrical power. Therefore, the allocated bandwidth for the k-th user is obtained by $B_k = \frac{B}{K}$.

As can be seen from Fig. 1(a), the input data of the k-th user are first split into N streams and each data stream is fed into an OFDMA encoder where DCO-OFDM modulation is performed. Subsequently, the outputs of N OFDMA encoders are used to drive N LEDs for simultaneous illumination and wireless communication. Letting $\mathbf{x} = [x_1, x_2, \ldots, x_N]^T$ be the transmitted electrical OFDM signal vector with a power of P_s, after free-space propagation, the received OFDM signal vector at the k-th user, i.e., $\mathbf{y}_k = [y_{k,1}, y_{k,2}, \ldots, y_{k,N}]^T$, can be expressed by

$$\mathbf{y}_k = \mathbf{H}_k \mathbf{x} + \mathbf{n}_k, \tag{1}$$

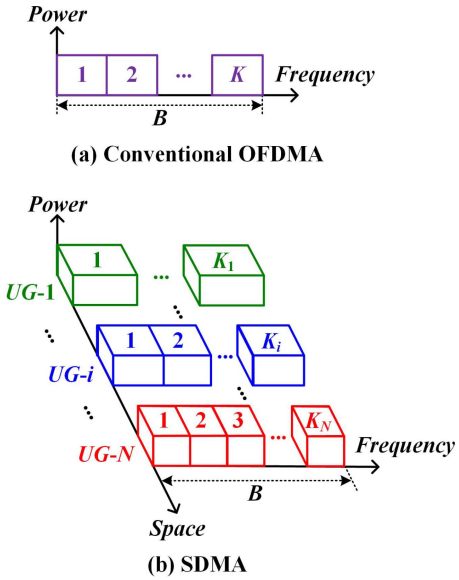

FIGURE 2. Illustration of resource allocation in a single-cell K-user $N \times N$ MIMO-VLC system using (a) conventional OFDMA and (b) SDMA with distributed user grouping.

where $\mathbf{H}_k$ is the $N \times N$ MIMO channel matrix for the k-th user and $\mathbf{n}_k = [n_{k,1}, n_{k,2}, \ldots, n_{k,N}]^T$ is the corresponding additive noise vector. The pre-estimated channel matrix $\mathbf{H}_k$ can be expressed by

$$\mathbf{H}_k = \begin{bmatrix} h_{k,11} & \cdots & h_{k,1N} \\ \vdots & \ddots & \vdots \\ h_{k,N1} & \cdots & h_{k,NN} \end{bmatrix}, \tag{2}$$

where the element $h_{k,ji}$ is the channel gain between the i-th ($i = 1, 2, \ldots, N$) LED and the j-th ($j = 1, 2, \ldots, N$) PD of the k-th user. As reported in [35], a time-multiplexed training approach can be adopted for efficient estimation of the channel matrix $\mathbf{H}_k$ in the MIMO-VLC system.

Assuming each LED follows a Lambertian radiation pattern and only considering the line-of-sight (LOS) components [16], the LOS channel gain is calculated by

$$h_{k,ji} = \frac{(m+1)\rho A}{2\pi d_{k,ji}^2} \cos^m\left(\varphi_{k,ji}\right) G_f G_l \cos\left(\theta_{k,ji}\right), \tag{3}$$

where m is the order of Lambertian emission which is defined by $m = -\ln 2/\ln(\cos(\Psi))$ with Ψ being the semi-angle at half power of each LED transmitter; ρ and A are the responsivity and the active area of the PD, respectively; $d_{k,ji}$ is the distance between the j-th PD of the k-th user and the i-th LED; $\varphi_{k,ji}$ and $\theta_{k,ji}$ are the corresponding emission angle and incident angle, respectively; G_f and G_l are the gains of the optical filter and the optical lens, respectively. The gain of the optical lens is given by $G_l = \frac{n^2}{\sin^2 \Phi}$, where n and Φ are the refractive index and the half-angle field-of-view (FOV) of the optical lens, respectively [2]. Note that the LOS channel gain becomes zero if the incident light is outside the FOV of the receiver.

Moreover, the additive noise consists of both thermal and shot noises which can be generally modeled as a real-valued zero-mean additive white Gaussian noise (AWGN) with power $P_n = N_0 B_m$, where N_0 is the power spectral density (PSD) of the additive noise and B_m is the modulation bandwidth [19].

To successfully decode the intended signal for the k-th user, MIMO de-multiplexing is first performed at the receiver side by using the estimated channel matrix. Due to its simplicity and low computational complexity, zero forcing (ZF) with basic channel inversion is adopted to perform MIMO de-multiplexing in the following analysis [36]. Hence, the transmitted OFDM signal vector for the k-th user can be estimated by multiplying the pseudo inverse (PI) of $\mathbf{H}_k$ with $\mathbf{y}_k$:

$$\hat{\mathbf{x}}_k = \mathbf{H}_k^{\star} \mathbf{y}_k = \mathbf{x} + \mathbf{H}_k^{\star} \mathbf{n}_k, \tag{4}$$

where the PI of $\mathbf{H}_k$, i.e., $\mathbf{H}_k^{\star}$, is given by

$$\mathbf{H}_k^{\star} = \left(\mathbf{H}_k^* \mathbf{H}_k\right)^{-1} \mathbf{H}_k^*. \tag{5}$$

In (5), $\mathbf{H}_k^*$ is the conjugated transpose of $\mathbf{H}_k$ and $(\cdot)^{-1}$ denotes the inverse of a matrix.

According to (4) and (5), the estimate of the i-th data stream corresponding to the i-th LED for the k-th user is obtained by

$$\hat{x}_{k,i} = x_i + \sum_{j=1}^{N} \widetilde{h}_{k,ij} n_{k,j}, \tag{6}$$

where $\widetilde{h}_{k,ij}$ is the element in the i-th row and the j-th column of $\mathbf{H}_k^{\star}$. Subsequently, OFDMA decoding is performed and the output data of the k-th user can be obtained by combining all the recovered N data streams together.

B. ACHIEVABLE RATE

Based on (6), the SNR of $\hat{x}_{k,i}$ can be calculated by

$$\gamma_{k,i} = \frac{P_s}{\sum_{j=1}^{N} \widetilde{h}_{k,ij}^2 P_n} = \frac{\gamma_{\text{tx}}}{\sum_{j=1}^{N} \widetilde{h}_{k,ij}^2}, \tag{7}$$

where $\gamma_{\text{tx}} = \frac{P_s}{P_n}$ denotes the transmit SNR. In typical MIMO-VLC systems, the received SNRs of different channels might be different due to different transmission paths. Hence, it is difficult to use received SNR as the metric to evaluate the performance of MIMO-VLC systems. Instead, transmitter SNR is the same for all the channels and hence allows a fair performance comparison as discussed in [19]. Therefore, transmit SNR is adopted in the following analysis.

Due to the average and peak power constraints and the non-negativity of the modulated optical signal, the classic Shannon equation is not applicable for achievable rate calculation in typical VLC systems and the exact capacity calculation of the VLC channel still remains a challenging open question. Nevertheless, several upper and lower bounds have been derived in literature. Here, we adopt the lower bound derived in [37] as an approximation of the

capacity of the VLC channel. Therefore, following [37], the achievable rate of the i-th data stream of the k-th user can be approximated by

$$R_{k,i} = \frac{1}{2} B_k \log_2\left(1 + \frac{e}{2\pi}\gamma_{k,i}\right), \tag{8}$$

where $B_k = \frac{B}{K}$. Hence, the achievable rate of the k-th user in the K-user $N \times N$ MIMO-VLC system using conventional OFDMA is given by the summation of the achievable rates of all the N data streams:

$$R_k = \sum_{i=1}^{N} R_{k,i} = \frac{B}{2K} \sum_{i=1}^{N} \log_2\left(1 + \frac{e}{2\pi}\gamma_{k,i}\right). \tag{9}$$

Consequently, the achievable sum rate of all the K users in the $N \times N$ MIMO-VLC system using conventional OFDMA is obtained by

$$\begin{aligned} \mathbb{R} &= \sum_{k=1}^{K} R_k \\ &= \frac{B}{2K} \sum_{k=1}^{K} \sum_{i=1}^{N} \log_2\left(1 + \frac{e\gamma_{\text{tx}}}{2\pi \sum_{j=1}^{N} \widetilde{h}_{k,ij}^2}\right). \end{aligned} \tag{10}$$

III. MIMO-VLC USING SDMA

It can be observed from Fig. 2(a) that the overall modulation bandwidth of the K-user $N \times N$ MIMO-VLC system is shared by all the K users. As a result, the available bandwidth of each user is relatively small, which limits both the achievable rate of each user and the sum rate of all users, especially when there are a relatively large number of users within the system coverage. To increase the available bandwidth of each user and hence improve the achievable rate/sum rate, we propose a novel multiple access technique, i.e., SDMA, for practical indoor single-cell MIMO-VLC systems. In the following, the principle of SDMA and the corresponding theoretical derivations are presented for a general MIMO-VLC system with an arbitrary number of users K and an arbitrary LED layout with N LEDs.

A. PRINCIPLE OF SDMA

The schematic diagram of an indoor K-user $N \times N$ MIMO-VLC system using SDMA with distributed user grouping (DUG) is illustrated in Fig. 1(b). As we can see, the input data of the k-th user is only transmitted by a single LED when using SDMA, whereas all the N LEDs are used to transmit the input data of the k-th user in conventional OFDMA. Particularly, the selection of a specific LED for the k-th user is based on the proposed DUG approach, which has a vital impact on the performance of SDMA. The detailed procedures to perform DUG will be discussed in Section III-B. At the receiver side, the output data of the OFDMA decoder which is corresponding to the specific LED assigned to the k-th user is selected as the output data of the k-th user.

For a K-user $N \times N$ MIMO-VLC system using SDMA with DUG in a practical indoor environment, all the K users are divided into totally N groups and the i-th UG, i.e., *UG-i*, consists of K_i users with $\sum_{i=1}^{N} K_i = K$. Each UG is corresponding to a specific LED in the ceiling and the number of UGs is exactly the same as the number of LEDs in the MIMO-VLC system. The resource allocation strategy of SDMA is shown in Fig. 2(b), where different UGs can be distinguished in the spatial domain and each UG can use the overall modulation bandwidth B of the MIMO-VLC system.

B. DISTRIBUTED USER GROUPING

Based on the above discussions, it can be found that user grouping plays an important role in SDMA based indoor single-cell MIMO-VLC systems. In the following, we further propose two DUG approaches to efficiently group users with different spatial locations. The fundamental principle of the proposed DUG approaches is to group users based on their SNR conditions with respect to different LEDs. It should be noted that each UG is corresponding to a specific LED and all the users within this UG will receive their intended signals from this specific LED, while treating the unintended signals from other LEDs as interference. This is quite different from the conventional OFDMA technique, where each user receives the intended signals from all the LEDs in the MIMO-VLC system [19].

Specifically, when there is only a single user within the i-th UG, i.e., $K_i = 1$, this user can use the entire modulation bandwidth B for signal transmission. Moreover, when there are multiple users within the i-th UG, i.e., $K_i > 1$, the OFDMA technique can be adopted for intra-UG multiple access. For the i-th UG with $K_i \geq 1$ users, the overall modulation bandwidth B is shared by these K_i users. Similarly, by assuming equal bandwidth allocation, the available bandwidth of the k-th user in the i-th UG is then given by $B_{k,i} = \frac{B}{K_i}$. However, there exist a special case that there might be no users within the i-th UG, i.e., $K_i = 0$. For better clarity of description, we here name the LED corresponding to an empty UG as an *idle LED* while the LED corresponding to a non-empty UG as a *serving LED*. When there are idle LEDs in the system, proper manners should be developed to handle these idle LEDs. Generally, for $K_i \geq 0$, two DUG approaches are proposed for SDMA based MIMO-VLC systems in the following, including basic DUG and transmit diversity-enhanced DUG.

1) BASIC DUG

In order to determine the specific UG that the k-th user belongs to, we first refer to the SNR of $\hat{x}_{k,i}$, i.e., $\gamma_{k,i}$ as derived by (7). Then, we can obtain the corresponding SNR vector $\mathbf{\Gamma}_k$ for the k-th user as follows

$$\mathbf{\Gamma}_k = \left[\gamma_{k,1}, \gamma_{k,2}, \ldots, \gamma_{k,N}\right], \tag{11}$$

where the element $\gamma_{k,i}$ is with respect to the i-th LED. Based on (11), the index of the UG which the k-th user belongs to, i.e., I_k, can be identified by obtaining the index of the largest element of $\mathbf{\Gamma}_k$, i.e., the index of the specific LED

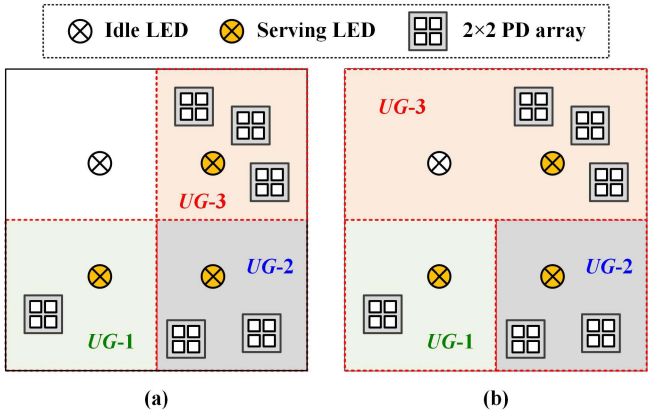

FIGURE 3. Illustration of (a) basic DUG and (b) TD-DUG in a single-cell 4 × 4 MIMO-VLC system using SDMA.

with respect to which a maximum SNR can be achieved by the k-th user:

$$I_k = \arg\max_i \ \gamma_{k,i}, \quad i \in \{1, 2, \ldots, N\}. \tag{12}$$

By utilizing (12), the k-th user can be assigned to its corresponding UG, i.e., $UG\text{-}I_k$, and therefore all the K users in the indoor $N \times N$ MIMO-VLC system can be successfully grouped. By counting the number of users assigned to each UG, we can obtain the values of K_i and further determine whether there are idle LEDs in the system or not.

In the basic DUG approach, the idle LEDs if any are simply deactivated for signal transmission and only DC biases are applied to maintain the illumination function. Without loss of generality, we assume that a subset of T $(0 \leq T < N)$ LEDs among the whole set of N LEDs are identified as idle LEDs, and hence the dimension of the channel matrix is changed to $N \times (N - T)$ and the resultant channel matrix $\mathbf{L}_k$ can be expressed by

$$\mathbf{L}_k = \left[\mathbf{l}_{k,1}, \mathbf{l}_{k,2}, \ldots, \mathbf{l}_{k,N-T}\right], \tag{13}$$

where the vector element $\mathbf{l}_{k,q} = [l_{k,1q}, l_{k,2q}, \ldots, l_{k,Nq}]^T$ is corresponding to the q-th $(q = 1, 2, \ldots, N - T)$ serving LED.

As per (13), $\mathbf{L}_k$ will become a $N \times 1$ vector if all the users are assigned to the same UG, which can be considered as an extreme case in the indoor $N \times N$ MIMO-VLC system. It is evident that simply deactivating the idle LEDs will lead to a substantial waste of resources since these LEDs are already there but not used for signal transmission.

2) TRANSMIT DIVERSITY-ENHANCED DUG

To fully explore the idle LEDs for capacity improvement of SDMA enabled MIMO-VLC systems, we further propose a transmit diversity-enhanced DUG (TD-DUG) approach. In TD-DUG, the idle LEDs are activated to transmit the intended signals for users. Particularly, an idle LED will be used to transmit the same signal as the LED which is the nearest from itself. Moreover, under the assumption of uniform LED distribution, there might be multiple LEDs which have the same shortest distance from an idle LED. In this scenario, the idle LED will transmit the same signal as the one which serves more users than others. Figs. 3(a) and (b) illustrate a single-cell 4×4 MIMO-VLC system using SDMA with basic DUG and TD-DUG, respectively. As shown in Fig. 3(a), the idle LED is simply deactivated for signal transmission when using SDMA with basic DUG. However, when using SDMA with TD-DUG, as shown in Fig. 3(b), the idle LED is also used for signal transmission. It can be seen that there are two LEDs, corresponding to UG-1 and UG-3, which have the same shortest distance to the idle LED. Since UG-3 consists of more users than UG-1, the idle LED is then used to transmit the same signal as the LED corresponding to UG-3 and hence provide transmit diversity for users within UG-3. Note that there exists the case that UG-1 and UG-3 contain the same number of users. In this case, the idle LED can be used to serve either UG-1 or UG-3. Considering the randomness of the spatial locations of users, the average sum rate achieved by assigning the idle LED to serve UG-1 or UG-3 should be comparable after averaging the obtained sum rates over multiple trails.

Following (11) and (12), the K users in the indoor $N \times N$ MIMO-VLC system is first grouped and the idle LEDs are then identified if any. Here, we assume that there are Z LEDs which have the same shortest distance from the t-th idle LED and each of them serves K_z users. Hence, the index of the LED, which the t-th idle LED will transmit the same signal as, can be obtained by

$$J_t = \arg\max_z \ K_z, \quad z \in \{1, 2, \ldots, Z\}. \tag{14}$$

Here, we assume there are a set of T_q idle LEDs transmit the same signal as the q-th serving LED with $\sum_{q=1}^{N-T} T_q = T$ and the corresponding channel matrix of these T_q idle LEDs at the k-th user is given by

$$\mathbf{W}_k = \left[\mathbf{w}_{k,1}, \mathbf{w}_{k,2}, \ldots, \mathbf{w}_{k,T_q}\right]. \tag{15}$$

Due to the negligible temporal delay between different LED-receiver links in practical indoor MIMO-VLC systems [19], the LOS channel gains corresponding to the q-th serving LED and those T_q idle LEDs can be directly added together at the k-th user. Therefore, the resultant $N \times (N - T)$ channel matrix using SDMA with TD-DUG can be obtained by

$$\mathbf{F}_k = \left[\mathbf{f}_{k,1}, \mathbf{f}_{k,2}, \ldots, \mathbf{f}_{k,N-T}\right], \tag{16}$$

where $\mathbf{f}_{k,q} = \mathbf{l}_{k,q} + \sum_{p=1}^{T_q} \mathbf{w}_{k,p}$ with $q = 1, 2, \ldots, N - T$.

Note that the successful realisation of the proposed DUG approaches in a practical MIMO-VLC system relies on a reliable uplink transmission, which can be achieved by adopting RF or infrared based uplink channels [38], [39].

C. TWO-STEP RESOURCE ALLOCATION

Based on the proposed DUG approaches, we further design a two-step resource allocation algorithm for SDMA enabled MIMO-VLC systems: the first step is inter-UG space allocation in the spatial domain according to DUG and the

Algorithm 1 Two-Step Resource Allocation for SDMA

```
Step 1: inter-UG space allocation
for k = 1 to K do
    Perform channel estimation as reported in [35]
    Estimate the SNR of each data stream
    Obtain Γ_k = [γ_{k,1}, γ_{k,2}, ..., γ_{k,N}]
    Find I_k using (12)
    Allocate user k to UG-I_k corresponding to LED I_k
end for
for i = 1 to N do
    Count the number of users, i.e., K_i, in UG-i
    if K_i = 0 then
        Deactivate the i-th LED if using basic DUG or
        activate the i-th LED for transmit diversity if using
        TD-DUG
    end if
end for
Step 2: intra-UG subcarrier allocation
for q = 1 to N − T do
    Divide M data subcarriers into K_q groups
    Allocate K_q subcarrier groups to K_q users respectively
end for
```

second step is intra-UG subcarrier allocation in the frequency domain based on the conventional OFDMA technique.

The detailed procedures of the two-step resource allocation algorithm is presented in Algorithm . For inter-UG space allocation, channel estimation with respect to each user is first performed as reported in [35], so as to obtain the corresponding channel matrix $\mathbf{H}_k$ for MIMO de-multiplexing. Then, the SNR of each data stream is estimated and the index of the UG for each user is identified by using (12). After that, all the K users in the $N \times N$ MIMO-VLC system can be successfully grouped and subsequently, the number of users in each UG is counted to obtain K_i. If $K_i = 0$, the corresponding i-th LED is either deactivated for signal transmission (if using basic DUG) or activated to achieve transmit diversity (if using TD-DUG). For intra-UG subcarrier allocation, the total M data subcarriers in the OFDM signal are divided into K_q groups and each group of data subcarriers are allocated to a respective user. Under the assumption of equal bandwidth allocation, the same number of data subcarriers will be allocated to each user within a UG, which is given by $\frac{M}{K_q}$.

D. ACHIEVABLE RATE

In the next, we derive the achievable rate of the k-th user and the achievable sum rate of all the K users in the indoor $N \times N$ MIMO-VLC system using the proposed SDMA technique with two different DUG approaches.

1) SDMA WITH BASIC DUG

When using SDMA with basic DUG, only $N - T$ serving LEDs transmit the intended signals for users while the T idle LEDs are not activated to transmit signal. For the k-th user in the I_k-th UG, only the I_k-th LED transmits the intended signal for the k-th user. Letting $x_k^\dagger$ be the intended electrical OFDM signal for the k-th user with power P_s, the transmitted electrical OFDM signal vector in the indoor MIMO-VLC system applying SDMA with basic DUG can be represented by $\mathbf{x}^\dagger = [x_1^\dagger, x_2^\dagger, \ldots, x_{N-T}^\dagger]^T$. As per (1) and (13), the received OFDM signal vector $\mathbf{y}_k^\dagger$ at the k-th user is given by

$$\mathbf{y}_k^\dagger = \mathbf{L}_k \mathbf{x}^\dagger + \mathbf{n}_k. \tag{17}$$

Subsequently, MIMO de-multiplexing is performed by using the PI of $\mathbf{L}_k$ and hence the estimate of $\mathbf{x}^\dagger$ is obtained by

$$\hat{\mathbf{x}}_k^\dagger = \mathbf{L}_k^\star \mathbf{y}_k^\dagger = \mathbf{x}^\dagger + \mathbf{L}_k^\star \mathbf{n}_k. \tag{18}$$

Since only the output of the I_k-th OFDMA decoder is intended for the k-th user, after output selection as shown in Fig. 1(b), the estimated of $x_{I_k}^\dagger$ can be expressed by

$$\hat{x}_{k,I_k}^\dagger = x_{I_k}^\dagger + \sum_{j=1}^{N} \widetilde{l}_{k,I_k j} n_{k,j}, \tag{19}$$

where $\widetilde{l}_{k,I_k j}$ denotes the element in the I_k-th row and the j-th column of $\mathbf{L}_k^\star$. Hence, the SNR of $\hat{x}_{k,I_k}^\dagger$ is calculated by

$$\gamma_{k,I_k}^\dagger = \frac{P_s}{\sum_{j=1}^{N} \widetilde{l}_{k,I_k j}^2 P_n} = \frac{\gamma_{\text{tx}}}{\sum_{j=1}^{N} \widetilde{l}_{k,I_k j}^2}. \tag{20}$$

Therefore, the achievable rate of the k-th user in the indoor $N \times N$ MIMO-VLC system using SDMA with basic DUG is obtained by

$$R_k^\dagger = \frac{1}{2} B_{k,I_k} \log_2\left(1 + \frac{e}{2\pi} \gamma_{k,I_k}^\dagger\right), \tag{21}$$

where $B_{k,I_k} = \frac{B}{K_{I_k}}$ with K_{I_k} being the number of users in the I_k-th UG. Finally, the achievable sum rate of all the K users using SDMA with basic DUG is given by the summation of the achievable rates of all the K users:

$$\begin{aligned} \mathbb{R}^\dagger &= \sum_{k=1}^{K} R_k^\dagger \\ &= \frac{B}{2} \sum_{k=1}^{K} \frac{1}{K_{I_k}} \log_2\left(1 + \frac{e\gamma_{\text{tx}}}{2\pi \sum_{j=1}^{N} \widetilde{l}_{k,I_k j}^2}\right). \end{aligned} \tag{22}$$

2) SDMA WITH TD-DUG

When using SDMA with TD-DUG, as discussed in Section III-B, the T idle LEDs are also activated for signal transmission in order to achieve transmit diversity. Accordingly, the received OFDM signal vector $\mathbf{y}_k^\ddagger$ at the k-th user using SDMA with TD-DUG is expressed by

$$\mathbf{y}_k^\ddagger = \mathbf{F}_k \mathbf{x}^\dagger + \mathbf{n}_k, \tag{23}$$

where $\mathbf{F}_k$ is the $N \times (N - T)$ channel matrix using SDMA with TD-DUG as in (16).

Following the steps from (17) to (22), we can respectively obtain the achievable rate of the k-th user and the achievable

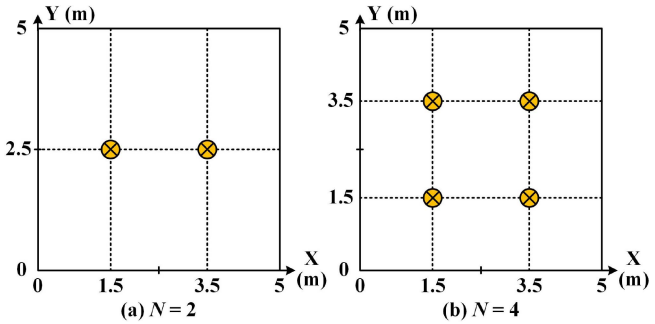

FIGURE 4. LED layouts in the ceiling for (a) $N = 2$ and (b) $N = 4$.

TABLE 1. Simulation parameters.

Parameter	Value
Room dimension	5 m × 5 m × 3 m
LED spacing	2 m
Semi-angle at half power of LED	70°
Gain of optical filter	0.9
Refractive index of optical lens	1.5
Half-angle FOV of optical lens	70°
PD spacing	5 cm
Responsivity of PD	0.53 A/W
Active area of PD	1 cm^2
Modulation scheme	BPSK
Modulation bandwidth	20 MHz
Noise power spectral density	10^{-22} A^2/Hz

sum rate of all the K users in the indoor $N \times N$ MIMO-VLC system using SDMA with TD-DUG as follows:

$$R_k^{\ddagger} = \frac{B}{2K_{I_k}} \log_2\left(1 + \frac{e\gamma_{\text{tx}}}{2\pi \sum_{j=1}^{N} \widetilde{f}_{k,I_k j}^2}\right), \tag{24}$$

$$\mathbb{R}^{\ddagger} = \frac{B}{2} \sum_{k=1}^{K} \frac{1}{K_{I_k}} \log_2\left(1 + \frac{e\gamma_{\text{tx}}}{2\pi \sum_{j=1}^{N} \widetilde{f}_{k,I_k j}^2}\right), \tag{25}$$

where $\widetilde{f}_{k,I_k j}$ denotes the element in the I_k-th row and the j-th column of $\mathbf{F}_k^{\star}$, which is the PI of $\mathbf{F}_k$ as given by (16).

IV. ANALYTICAL AND SIMULATION RESULTS

To verify the feasibility of applying SDMA with DUG for indoor multiuser MIMO-VLC systems, detailed analytical and simulation evaluations are performed in this section. Here, the K-user $N \times N$ MIMO-VLC system is configured in a practical indoor environment with a dimension of 5 m × 5 m × 3 m, where both 2×2 ($N = 2$) and 4×4 ($N = 4$) MIMO settings are considered in the following evaluations. The LED layouts in the ceiling for $N = 2$ and 4 are depicted in Figs. 4(a) and (b), respectively. For $N = 2$, the LEDs are located at (1.5 m, 2.5 m, 3 m) and (3.5 m, 2.5 m, 3 m), respectively. For $N = 4$, the LEDs are located at (1.5 m, 1.5 m, 3 m), (1.5 m, 3.5 m, 3 m), (3.5 m, 3.5 m, 3 m) and (3.5 m, 1.5 m, 3 m), respectively. As we can see, the spacing between two adjacent LEDs in both 2×2 and 4×4 MIMO settings is 2 m. The LEDs in the ceiling are oriented downwards to point straight to the receiving plane, while the PDs of each user in the receiving plane are vertically oriented towards the ceiling. The height of the receiving plane is fixed at 0.85 m unless otherwise specified.

The other key simulation parameters of the indoor MIMO-VLC system are listed in Table 1. The semi-angle at half power of each LED is 70°. The gain of the optical filter is 0.9. The refractive index and the half-angle FOV of the optical lens are 1.5 and 70°, respectively. Each PD has a responsivity of 0.53 A/W and an active area of 1 cm^2. The spacing between two adjacent PDs in both 2×2 and 4×4 MIMO settings is 5 cm. The overall modulation bandwidth of the MIMO-VLC system is set to 20 MHz and the noise PSD is assumed to be 10^{-22} A^2/Hz. Moreover, binary phase-shift keying (BPSK) based OFDM signals are transmitted by each LED in the simulation evaluations. The SNR value of each received OFDM signal is estimated from the error vector magnitude (EVM) of the corresponding BPSK constellation, which is then used to calculate the achievable rate.

Note that it is reasonable to assume a 20-MHz modulation bandwidth in the simulations, since various FDE schemes can be applied to extend the limited 3-dB modulation bandwidth of COTS white LEDs [11]–[13]. Moreover, by regulating the input signal within the dynamic range of the LED and applying various LED nonlinearity compensation techniques such as pre- or post-distortion and post-equalization [40]–[44], it is also reasonable to neglect the nonlinear effects of the LED in the simulations.

We first evaluate the achievable data rate of a specific user over the receiving plane in the K-user $N \times N$ MIMO-VLC system using conventional OFDMA and SDMA with DUG. Fig. 5(a) shows the achievable rate versus the X coordinate of the user in the 2×2 MIMO-VLC system, where there is only one user, i.e., $K = 1$, located at (X, 2.5 m, 0.85 m) over the receiving plane and the transmit SNR is $\gamma_{\text{tx}} = 150$ dB. When using the conventional OFDMA technique, the achievable rate of the user first increases with the increase of X and a maximum rate of 121.4 Mb/s is achieved at X = 2.5 m, i.e., the center of the room. With the further increase of X, the achievable rate of the user is then gradually reduced. However, when the proposed SDMA technique is applied in the 2×2 MIMO-VLC system, the achievable rate of the user is substantially improved. More specifically, when applying SDMA with basic DUG, the maximum rates of 149.7 Mb/s are obtained at X = 1.5 and 3.5 m, i.e., the user is located right under the two LEDs, and the achievable rate is reduced to 139.5 Mb/s at X = 2.5 m. The substantial achievable rate improvement is mainly due to the elimination of inter-channel interference in conventional OFDMA, since only one LED transmits the intended signal for the user by using SDMA with basic DUG. Moreover, when SDMA with TD-DUG is applied, the achievable rate of the user can be further greatly improved, especially around the central position of the room. Particularly, the achievable rate of the user is improved from 139.5 to 159.5 Mb/s at X = 2.5 m, indicating an achievable rate improvement of 14.3%. The further achievable rate improvement by applying SDMA with TD-DUG is due to the additional spatial diversity through

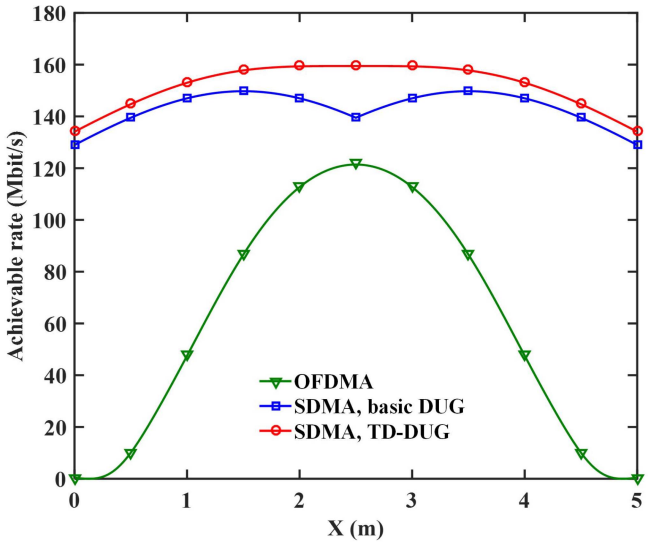

(a) $K = 1$

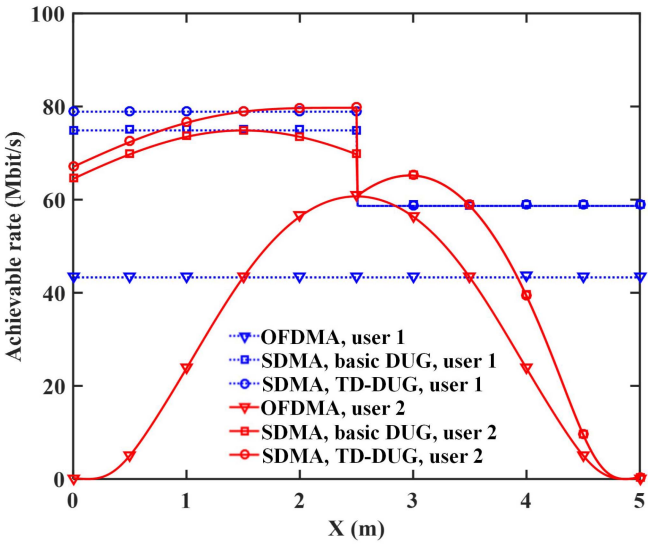

(b) $K = 2$

FIGURE 5. (a) Achievable rate versus the X coordinate of the user for $K = 1$ where the user is located at (X, 2.5 m, 0.85 m) in the 2 × 2 MIMO-VLC system and (b) achievable rate versus the X coordinate of user 2 for $K = 2$ where user 1 is fixed at (1.5 m, 2.5 m, 0.85 m) and user 2 is located at (X, 2.5 m, 0.85 m) in the 2 × 2 MIMO-VLC system. The transmit SNR is $\gamma_{tx} = 150$ dB. Lines and makers show the analytical and simulation results, respectively.

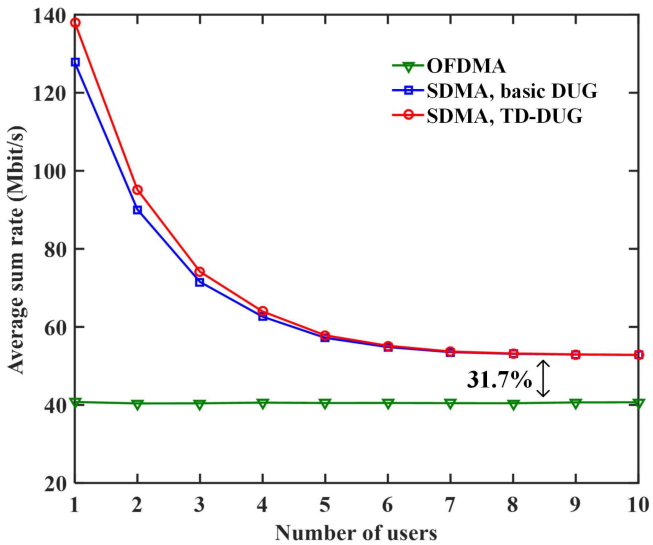

(a) $N = 2$

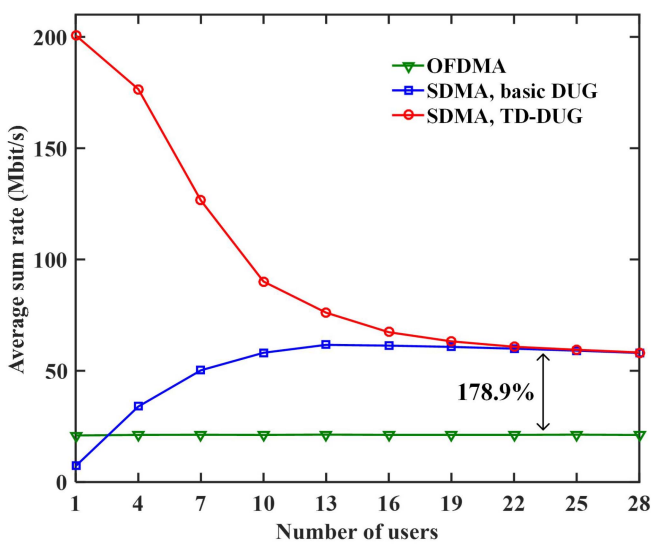

(b) $N = 4$

FIGURE 6. Average sum rate versus the number of users K for (a) $N = 2$ with $\gamma_{tx} = 150$ dB and (b) $N = 4$ with $\gamma_{tx} = 160$ dB.

activating the idle LED to transmit the same signal as the serving LED. The achievable rate versus the X coordinate of user 2 for $K = 2$ is shown in Fig. 5(b), where user 1 is fixed at (1.5 m, 2.5 m, 0.85 m) while user 2 is located at (X, 2.5 m, 0.85 m) with $\gamma_{tx} = 150$ dB. When using OFDMA, since user 1 has a fixed position, the achievable rate of user 1 remains the same for different X values, while the achievable rate of user 2 has the similar trend as the single user case in Fig. 5(a). In contrast, when using SDMA with either basic TUG or TD-DUG, user 1 achieves different rates for $X \leq 2.5$ and $X > 2.5$. For $X \leq 2.5$, user 1 and user 2 are serving by the same LED, and both will not receive interference from the idle LED. However, for $X > 2.5$, user 1 and user 2 are served by different LEDs and they will both receive interference from the adjacent LED. Moreover, TD-DUG outperforms basic DUG only for $X \leq 2.5$ since no transmit diversity can be exploited for $X > 2.5$. In Figs. 5(a) and (b), the analytical results and the simulation results are given by the lines and the markers, respectively. It can be clearly observed that the simulation results agree well with the analytical predictions, which successfully verifies the analytical derivations obtained in Section III.

In the next, we evaluate the achievable sum rate performance of the K-user $N \times N$ MIMO-VLC system using conventional OFDMA and SDMA with DUG, where the positions of the K users are randomly selected over the

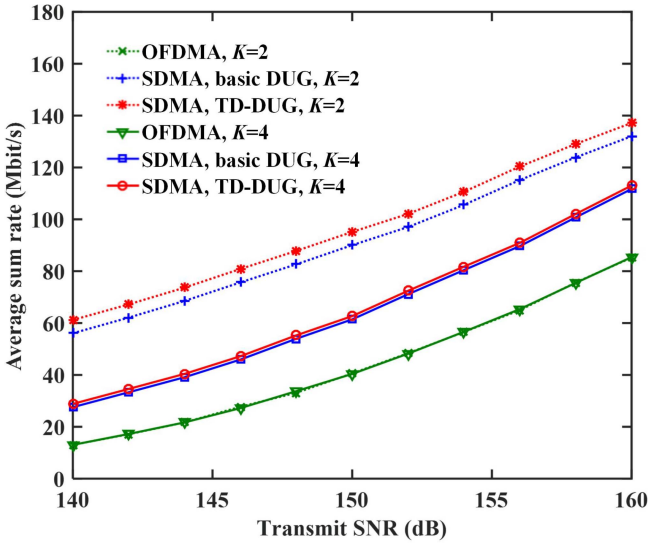

(a) $N = 2$

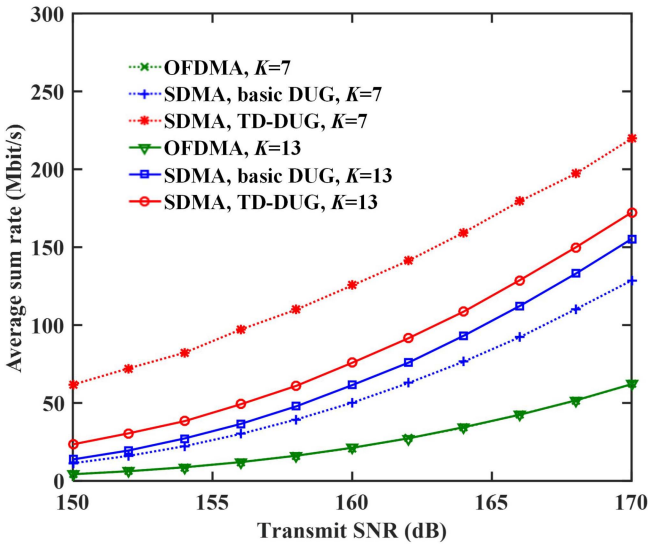

(b) $N = 4$

FIGURE 7. Average sum rate versus the transmit SNR γ_{tx} with different numbers of users for (a) $N = 2$ and (b) $N = 4$.

receiving plane. To obtain accurate sum rates, the simulations are repeated 10000 times and the obtained average sum rates are employed in the following evaluations. Figs. 6(a) and (b) show the average sum rate versus the number of users, i.e., K, for $N = 2$ with $\gamma_{tx} = 150$ dB and $N = 4$ with $\gamma_{tx} = 160$ dB, respectively. As we can see, when using conventional OFDMA, the achievable average sum rates remain stable for different K values for both $N = 2$ and 4, which are 40.4 and 21.3 Mb/s, respectively. However, for $N = 2$ using SDMA with either basic DUG or TD-DUG, as shown in Fig. 6(a), the achievable average sum rate first reduces as K is increased from 1 to 7, which then remains stable at 53.2 Mb/s as $K \geq 8$. This can be explained as follows: when K is relatively small, the probability that an idle LED occurs in the 2×2 MIMO-VLC system is high and hence SDMA can achieve much higher average sum rate than conventional OFDMA due to the elimination of inter-channel interference. Moreover, TD-DUG outperforms basic DUG for small K values because of the additional transmit diversity, and nearly the same rate performance can be achieved for basic DUG and TD-DUG as $K \geq 6$. Compared with conventional OFDMA, at least 31.7% average sum rate improvement can be achieved by using SDMA with either basic DUG or TD-DUG for $N = 2$ with $\gamma_{tx} = 150$ dB. For $N = 4$ with $\gamma_{tx} = 160$ dB, as shown in Fig. 6(b), the average sum rate using SDMA with TD-DUG has a similar trend as that for $N = 2$, while the average sum rate using SDMA with basic DUG has a different trend, which gradually increases as K is increased from 1 to 13 and then remains stable as $K \geq 13$. The change of trend of SDMA with basic DUG for $N = 4$ be explained as follows: with the increase of N, more idle LEDs will occur when K is relatively small, which can significantly reduce the achievable sum rate. Nevertheless, when K becomes large, less idle LEDs will occur and hence SDMA with either basic DUG or TD-DUG significantly outperforms conventional OFDMA by 178.9% in terms of average sum rate. It can be seen from Figs. 6(a) and (b) that the rate improvements using SDMA over OFDMA will remain stable when the number of users is relatively large, and a much more significant rate improvement can be achieved when N is increased from 2 to 4.

We further evaluate the relationship between the achievable sum rate and the transmit SNR in the K-user $N \times N$ MIMO-VLC system. Figs. 7(a) and (b) show the average sum rate versus the transmit SNR γ_{tx} with different numbers of users for $N = 2$ and 4, respectively. For $N = 2$ with $K = 2$, the largest average sum rate is achieved by SDMA with TD-DUG, which outperforms SDMA with basic DUG by about 5 Mb/s as the transmit SNR is in the range of 140 to 160 dB. For $N = 2$ with $K = 4$, nearly the same average sum rates are obtained using SDMA with basic DUG and TD-DUG. The lowest average sum rates are achieved by OFDMA which are the same for $K = 2$ and 4. When N is increased to 4, the average sum rate improvement by using TD-DUG in SDMA over basic DUG becomes much more significant for $K = 7$ due to high transmit diversity.

V. EXPERIMENTAL RESULTS

Besides the above analytical and simulation evaluations, a proof-of-concept experiment is further demonstrated to compare the performance of the conventional OFDMA and the proposed SDMA technique in a practical MIMO-VLC system. In the experiments, we consider a 2×2 MIMO-VLC system with K users for performance comparison.

The experimental setup of the single-cell MIMO-VLC system is shown in Fig. 8(a), where two channels of OFDM signals are generated offline by MATLAB and then uploaded to an arbitrary waveform generator (AWG, Tabor WW2074) with a sampling rate of 50 MSa/s. After that, two analog bipolar signals are obtained and two 250-mA DC bias

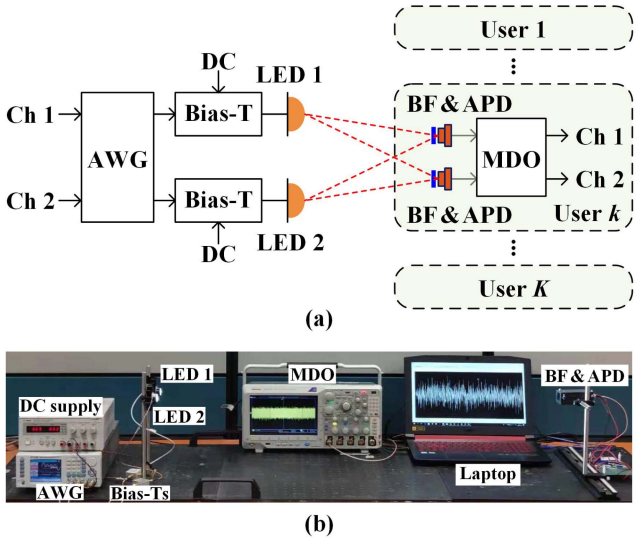

FIGURE 8. (a) Experimental setup and (b) photo of the experimental testbed.

TABLE 2. Experimental parameters.

Parameter	Value
AWG sampling rate	50 MSa/s
DC bias current	250 mA
LED spacing	10 cm
APD spacing	3 cm
Responsivity of APD	15 A/W at 450 nm
Active area of APD	19.6 mm^2
MDO sampling rate	250 MSa/s
Modulation scheme	BPSK
IFFT/FFT size	512
Modulation bandwidth	20 MHz
Transmission distance	100∼120 cm

currents are further added through two bias-tees (bias-Ts) to ensure the non-negativity of the LED-driven signals. Subsequently, the resultant signals are utilized to drive two commercial off-the-shelf white LEDs (Luxeon Star). After free-space propagation, the radiated light is detected by the K users where each user is equipped with two blue filters (BFs) and two avalanche photodiodes (APDs, Hamamatsu S8664-50K). The APDs have a responsivity of 15 A/W at 450 nm and an active area of 19.6 mm^2. At each user, the detected signals are sampled by a mixed domain oscilloscope (MDO, Tektronix MDO3104) at 250 MSa/s and the digitized signals are further processed offline. The photo of the experimental testbed is depicted in Fig. 8(b). Due to the hardware limitation, we adjust the position of the APD to detect the two channels of OFDM signals for each user.

The two digital OFDM signals are generated offline with an inverse fast Fourier transform (IFFT) size of 512, where totally 205 (2-nd to 206-th) subcarriers are used to carry valid data. As a result, the effective bandwidth of each OFDM signal is about 20 MHz. Moreover, BPSK constellation is adopted in the OFDM modulation which is used for SNR estimation and achievable rate calculation. The key experimental parameters are summarized in Table 2.

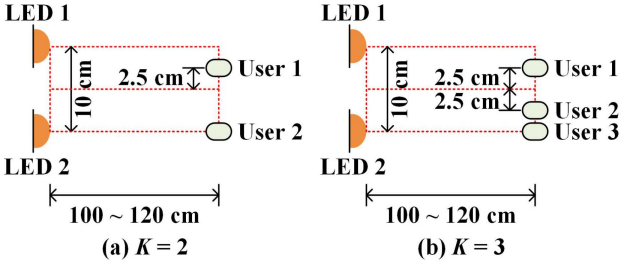

FIGURE 9. Geometric setup for (a) $K = 2$ and (b) $K = 3$.

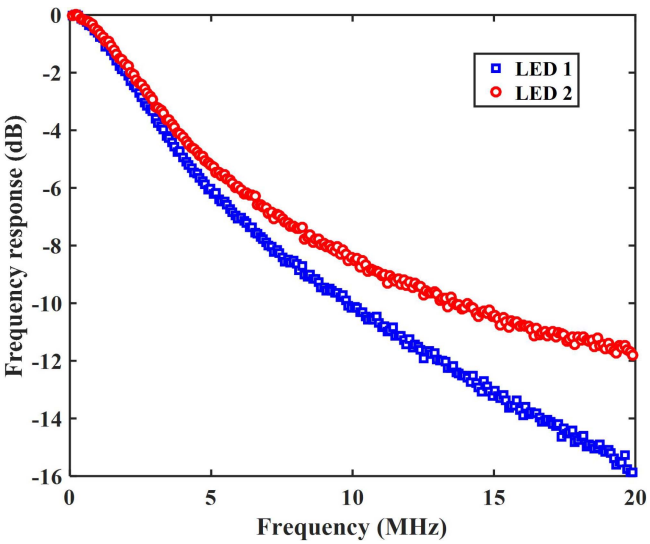

FIGURE 10. Measured frequency responses of the LEDs with blue filtering.

Figs. 9(a) and (b) illustrate two geometric setups adopted in this experimental demonstration for $K = 2$ and 3, respectively. The spacing between the two LEDs is set to 10 cm and the transmission distance is ranged from 100 to 120 cm with a step of 5 cm. For each user, the spacing between two APDs is set to 3 cm. For $K = 2$, as can be seen from Fig. 9(a), user 1 and user 2 are individually served by LED 1 and LED 2, respectively, when using SDMA. For $K = 3$, as can be seen from Fig. 9(b), user 1 is individually served by LED 1 while user 2 and user 3 are allocated in the same UG which is served by LED 2. For both two geometric setups, there are no idle LEDs and hence basic DUG and TD-DUG become the same when applying SDMA in the demonstrated system.

Fig. 10 depicts the measured frequency responses of the two LEDs with blue filtering. As we can see, the 3-dB modulation bandwidth of these LEDs after applying blue filters is only about 3 MHz. Moreover, for a 20-MHz bandwidth, the power attenuations of LED 1 and LED 2 reach 15.9 and 11.8 dB, respectively. Since OFDMA is adopted for intra-UG multiple access in the proposed SDMA technique, it is necessary to achieve a relatively flat frequency response with respect to each LED. As a result, digital pre-frequency domain equalization (pre-FDE) is performed here and its principle can be found in [13]. Fig. 11 compares the

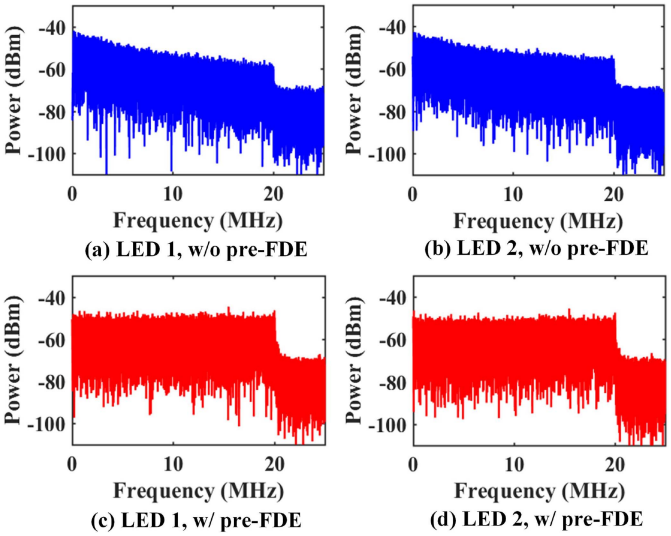

FIGURE 11. Received electrical spectra with respect to (a) LED 1 without pre-FDE, (b) LED 2 without pre-FDE, (c) LED 1 with pre-FDE, and (d) LED 2 with pre-FDE.

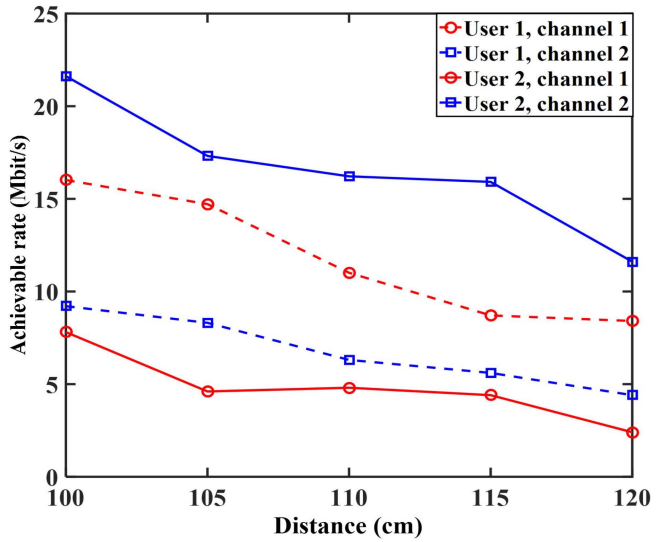

FIGURE 12. Measured achievable rate versus transmission distance for different channels of different users using OFDMA with $K = 2$.

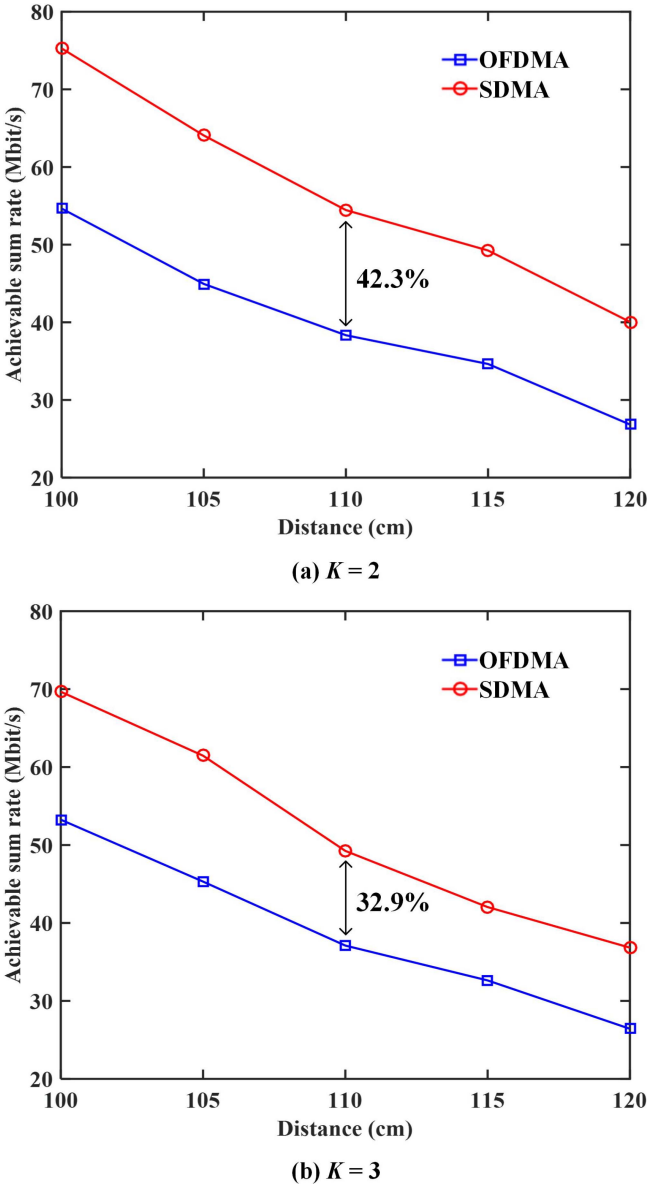

FIGURE 13. Measured sum rate versus transmission distance using conventional OFDMA and the proposed SDMA for (a) $K = 2$ and (b) $K = 3$.

received electrical spectra with respect to LED 1 and LED 2 without and with pre-FDE. As we can observe, compared with the received electrical spectra without pre-FDE which have significant power attenuations, two significantly flattened spectra with respect to both LEDs can be obtained after performing pre-FDE. Due to the different frequency responses of two LEDs, the applied peak-to-peak voltages in the AWG for LED 1 and LED 2 are set to 5 and 3 V, respectively.

Fig. 12 shows the measured achievable rate versus transmission distance for different channels of different users using OFDMA with $K = 2$. As we can see, there exists certain rate difference between different channels of the same user. For user 1, the achievable rate of channel 1 is relatively higher than that of channel 2, which is because user 1 is more close to LED 1 and hence channel 1 has better SNR performance than channel 2. For user 2, channel 2 achieves much higher rate than that of channel 1, and the rate difference between channel 1 and channel 2 of user 2 is more significant than that of user 1, which is due to the fact that user 2 has a larger position offset from the center of the LED array than user 1. Hence, the rate difference is related to the position of the user. When SDMA is adopted, the rate difference of different channels can be eliminated since each user only receives signal from a single LED, and hence the achievable sum rate can be improved.

Figs. 13(a) and (b) show the measured sum rate of K users versus the transmission distance of the 2×2 MIMO-VLC system for $K = 2$ and 3, respectively. Considering that SDMA with basic DUG and SDMA with TD-DUG become

exactly the same under the geometric setup shown in Fig. 9, we simply use "SDMA" to represent both "SDMA with basic DUG" and "SDMA with TD-DUG" and compare it with "OFDMA". It can be seen that the achievable sum rates are gradually reduced with the increase of transmission distance for both $K = 2$ and 3. Specifically, for $K = 2$, the achievable sum rate is 38.3 Mbit/s at the distance of 110 cm when applying the conventional OFDMA. However, the achievable sum rate at the distance of 110 cm is increased to 54.5 Mbit/s when employing the proposed SDMA technique, which indicates a sum rate improvement of 42.3% in comparison to the conventional OFDMA. Moreover, for $K = 3$, the sum rate improvement at the distance of 110 cm using SDMA over conventional OFDMA is slightly reduced to 32.9%, which is in accordance with the observation of the analytical results shown in Fig. 6 that the rate improvement will be reduced with the increase in the total number of users when the total number of users is relatively small. Evidently, the obtained experimental results can verify the superiority of applying the proposed SDMA technique for substantial achievable sum rate improvement in practical indoor MIMO-VLC systems.

VI. CONCLUSION

In this paper, we have proposed, analyzed and demonstrated a novel SDMA technique for indoor spatial multiplexing-based multi-user MIMO-VLC systems. By exploiting the spatial distributions of users over the receiving plane with respect to LED transmitters in the ceiling, the users are divided into multiple UGs and each UG can access the overall modulation bandwidth of the MIMO-VLC system. Compared with the conventional OFDMA based MIMO-VLC systems where the overall modulation bandwidth is divided and shared by all the users, much more efficient bandwidth utilization is achieved in SDMA based MIMO-VLC systems. Two DUG approaches (i.e., basic DUG and TD-DUG) have been proposed and a two-step resource allocation algorithm has also been designed for the implementation of SDMA in practical MIMO-VLC systems. The feasibility and superiority of applying SDMA in indoor MIMO-VLC systems have been successfully verified by both analytical and simulation results and proof-of-concept experimental results. The obtained results demonstrate that the proposed SDMA technique can substantially improve the achievable sum rate of practical MIMO-VLC systems when compared with the widely used OFDMA technique.

REFERENCES

[1] S. Pimputkar, J. S. Speck, S. P. DenBaars, and S. Nakamura, "Prospects for LED lighting," *Nat. Photon.*, vol. 3, no. 4, pp. 180–182, Apr. 2009.

[2] T. Komine and M. Nakagawa, "Fundamental analysis for visible-light communication system using LED lights," *IEEE Trans. Consum. Electron.*, vol. 50, no. 1, pp. 100–107, Feb. 2004.

[3] D. Karunatilaka, F. Zafar, V. Kalavally, and R. Parthiban, "LED based indoor visible light communications: State of the art," *IEEE Commun. Surveys Tuts.*, vol. 17, no. 3, pp. 1649–1678, 3rd Quart., 2015.

[4] H. Haas, "Visible light communication," in *Proc. Opt. Fiber Commun. Conf. (OFC)*, Mar. 2015, pp. 1–3.

[5] H. Haas, L. Yin, Y. Wang, and C. Chen, "What is LiFi?" *J. Lightw. Technol.*, vol. 34, no. 6, pp. 1533–1544, Mar. 15, 2016.

[6] L. Grobe *et al.*, "High-speed visible light communication systems," *IEEE Commun. Mag.*, vol. 51, no. 12, pp. 60–66, Dec. 2013.

[7] J. Armstrong, Y. Sekercioglu, and A. Neild, "Visible light positioning: A roadmap for international standardization," *IEEE Commun. Mag.*, vol. 51, no. 12, pp. 68–73, Dec. 2013.

[8] P. H. Pathak, X. Feng, P. Hu, and P. Mohapatra, "Visible light communication, networking, and sensing: A survey, potential and challenges," *IEEE Commun. Surveys Tuts.*, vol. 17, no. 4, pp. 2047–2077, 4th Quart., 2015.

[9] D. Wu, W.-D. Zhong, Z. Ghassemlooy, and C. Chen, "Short-range visible light ranging and detecting system using illumination light emitting diodes," *IET Optoelectron.*, vol. 10, no. 3, pp. 94–99, Jun. 2016.

[10] S. Rajagopal, R. D. Roberts, and S.-K. Lim, "IEEE 802.15.7 visible light communication: Modulation schemes and dimming support," *IEEE Commun. Mag.*, vol. 50, no. 3, pp. 72–82, Mar. 2012.

[11] H. Le Minh *et al.*, "100-Mb/s NRZ visible light communications using a postequalized white LED," *IEEE Photon. Technol. Lett.*, vol. 21, no. 15, pp. 1063–1065, Aug. 2009.

[12] Y.-F. Liu, Y. C. Chang, C.-W. Chow, and C.-H. Yeh, "Equalization and pre-distorted schemes for increasing data rate in in-door visible light communication system," in *Proc. Opt. Fiber Commun. Conf. (OFC)*, Los Angeles, CA, USA, Mar. 2011, pp. 1–3.

[13] C. Chen, W.-D. Zhong, and D. Wu, "Indoor OFDM visible light communications employing adaptive digital pre-frequency domain equalization," in *Proc. Conf. Lasers Electro Opt. (CLEO)*, San Jose, CA, USA, Jun. 2016, pp. 1–2.

[14] D. Tsonev *et al.*, "A 3-Gb/s single-LED OFDM-based wireless VLC link using a gallium nitride μLED," *IEEE Photon. Technol. Lett.*, vol. 26, no. 7, pp. 637–640, Apr. 2014.

[15] Y. Yang *et al.*, "Secure and private NOMA VLC using OFDM with two-level chaotic encryption," *Opt. Exp.*, vol. 26, no. 26, pp. 34031–34042, Dec. 2018.

[16] L. Zeng *et al.*, "High data rate multiple input multiple output (MIMO) optical wireless communications using white LED lighting," *IEEE J. Sel. Areas Commun.*, vol. 27, no. 9, pp. 1654–1662, Dec. 2009.

[17] C. Chen, W.-D. Zhong, H. Yang, and P. Du, "On the performance of MIMO-NOMA-based visible light communication systems," *IEEE Photon. Technol. Lett.*, vol. 30, no. 4, pp. 307–310, Feb. 15, 2018.

[18] C. Chen, W.-D. Zhong, and D. Wu, "On the coverage of multiple-input multiple-output visible light communications [Invited]," *IEEE/OSA J. Opt. Commun. Netw.*, vol. 9, no. 9, pp. D31–D41, Sep. 2017.

[19] T. Fath and H. Haas, "Performance comparison of MIMO techniques for optical wireless communications in indoor environments," *IEEE Trans. Commun.*, vol. 61, no. 2, pp. 733–742, Feb. 2013.

[20] A. H. Azhar, T. Tran, and D. O'Brien, "A gigabit/s indoor wireless transmission using MIMO-OFDM visible-light communications," *IEEE Photon. Technol. Lett.*, vol. 25, no. 2, pp. 171–174, Jan. 2013.

[21] T. Q. Wang, Y. A. Sekercioglu, and J. Armstrong, "Analysis of an optical wireless receiver using a hemispherical lens with application in MIMO visible light communications," *J. Lightw. Technol.*, vol. 31, no. 11, pp. 1744–1754, Jun. 1, 2013.

[22] T. Chen, L. Liu, B. Tu, Z. Zheng, and W. Hu, "High-spatial-diversity imaging receiver using fisheye lens for indoor MIMO VLCs," *IEEE Photon. Technol. Lett.*, vol. 26, no. 22, pp. 2260–2263, Nov. 2014.

[23] C. Chen, W.-D. Zhong, D. Wu, and Z. Ghassemlooy, "Wide-FOV and high-gain imaging angle diversity receiver for indoor SDM-VLC systems," *IEEE Photon. Technol. Lett.*, vol. 28, no. 19, pp. 2078–2081, Oct. 1, 2016.

[24] S.-B. Li, C. Gong, P. Wang, and Z. Xu, "Lens design for indoor MIMO visible light communications," *Opt. Commun.*, vol. 389, pp. 224–229, Apr. 2017.

[25] Y. Hong, J. Chen, Z. Wang, and C. Yu, "Performance of a precoding MIMO system for decentralized multiuser indoor visible light communications," *IEEE Photon. J.*, vol. 5, no. 4, Aug. 2013, Art. no. 7800211.

[26] Y. Fan, Q. Zhao, B. Kang, and L. Deng, "Equivalent ZF precoding scheme for downlink indoor MU-MIMO VLC systems," *Opt. Commun.*, vol. 407, pp. 402–409, Jan. 2018.

[27] K. Ying, Z. Yu, R. J. Baxley, H. Qian, G.-K. Chang, and G. T. Zhou, "Nonlinear distortion mitigation in visible light communications," *IEEE Wireless Commun.*, vol. 22, no. 2, pp. 36–45, Apr. 2015.

[28] J.-Y. Sung, C.-H. Yeh, C.-W. Chow, W.-F. Lin, and Y. Liu, "Orthogonal frequency-division multiplexing access (OFDMA) based wireless visible light communication (VLC) system," *Opt. Commun.*, vol. 355, pp. 261–268, Nov. 2015.

[29] M. Hammouda, A. M. Vegni, H. Haas, and J. Peissig, "Resource allocation and interference management in OFDMA-based VLC networks," *Phys. Commun.*, vol. 31, pp. 169–180, Dec. 2018.

[30] S.-M. Kim and H.-J. Lee, "Visible light communication based on space-division multiple access optical beamforming," *Chin. Opt. Lett.*, vol. 12, no. 12, Dec. 2014, Art no. 120601.

[31] Z. Chen, D. A. Basnayaka, and H. Haas, "Space division multiple access for optical attocell network using angle diversity transmitters," *J. Lightw. Technol.*, vol. 35, no. 11, pp. 2118–2131, Jun. 1, 2017.

[32] O. González, M. F. Guerra-Medina, I. R. Martín, F. Delgado, and R. Pérez-Jiménez, "Adaptive WHTS-assisted SDMA-OFDM scheme for fair resource allocation in multi-user visible light communications," *J. Opt. Commun. Netw.*, vol. 8, no. 6, pp. 427–440, Jun. 2016.

[33] C. Chen *et al.*, "NOMA for MIMO visible light communications: A spatial domain perspective," in *Proc. IEEE Global Commun. Conf. (GLOBECOM)*, Waikoloa, HI, USA, Dec. 2019, pp. 1–6.

[34] J. Armstrong and B. J. Schmidt, "Comparison of asymmetrically clipped optical OFDM and DC-biased optical OFDM in AWGN," *IEEE Commun. Lett.*, vol. 12, no. 5, pp. 343–345, May 2008.

[35] Y. Wang and N. Chi, "Demonstration of high-speed 2×2 non-imaging MIMO Nyquist single carrier visible light communication with frequency domain equalization," *J. Lightw. Technol.*, vol. 32, no. 11, pp. 2087–2093, Jun. 1, 2014.

[36] A. Burton, H. Minh, Z. Ghassemlooy, E. Bentley, and C. Botella, "Experimental demonstration of 50-Mb/s visible light communications using 4×4 MIMO," *IEEE Photon. Technol. Lett.*, vol. 26, no. 9, pp. 945–948, May 2014.

[37] A. Lapidoth, S. M. Moser, and M. A. Wigger, "On the capacity of free-space optical intensity channels," *IEEE Trans. Inf. Theory*, vol. 55, no. 10, pp. 4449–4461, Oct. 2009.

[38] M. Ayyash *et al.*, "Coexistence of WiFi and LiFi toward 5G: Concepts, opportunities, and challenges," *IEEE Commun. Mag.*, vol. 54, no. 2, pp. 64–71, Feb. 2016.

[39] M. D. Soltani, X. Wu, M. Safari, and H. Haas, "Bidirectional user throughput maximization based on feedback reduction in LiFi networks," *IEEE Trans. Commun.*, vol. 66, no. 7, pp. 3172–3186, Jul. 2018.

[40] R. Mitra and V. Bhatia, "Chebyshev polynomial-based adaptive predistorter for nonlinear LED compensation in VLC," *IEEE Photon. Technol. Lett.*, vol. 28, no. 10, pp. 1053–1056, May 15, 2016.

[41] X. Deng, S. Mardanikorani, K. Arulandu, and J.-P. M. Linnartz, "Novel post-distortion to mitigate LED nonlinearity in high-speed visible light communications," in *Proc. IEEE Globecom Workshops (GC Wkshps)*, Abu Dhabi, UAE, Dec. 2018, pp. 1–6.

[42] G. Stepniak, J. Siuzdak, and P. Zwierko, "Compensation of a VLC phosphorescent white LED nonlinearity by means of Volterra DFE," *IEEE Photon. Technol. Lett.*, vol. 25, no. 16, pp. 1597–1600, Aug. 2013.

[43] C. Chen, X. Deng, Y. Yang, P. Du, H. Yang, and L. Zhao, "LED nonlinearity estimation and compensation in VLC systems using probabilistic Bayesian learning," *Appl. Sci.*, vol. 9, no. 13, p. 2711, Jan. 2019.

[44] X. Lu *et al.*, "Memory-controlled deep LSTM neural network post-equalizer used in high-speed PAM VLC system," *Opt. Exp.*, vol. 27, no. 5, pp. 7822–7833, Mar. 2019.